



## Laboratory modeling and analysis of slopes of different geometry under the effect of precipitation

Mert Takci<sup>1</sup>, Inci Develioglu<sup>1</sup>, Hasan Firat Pulat<sup>\*1</sup>, Hasan Emre Demirci<sup>1</sup>

<sup>1</sup>Izmir Katip Celebi University, Department of Civil Engineering, Türkiye

### Keywords

Laboratory model  
Plaxis 2D  
Precipitation  
Slope angle  
Slope stability

### Research Article

DOI: 10.31127/tuje.1191246

Received:18.10.2022

Revised: 04.03.2022

Accepted: 07.03.2022

Published:24.04.2023



### Abstract

Back stability analysis, in-lab testing, and field tests may all be used to assess the behavior of stability of slopes. Each of these approaches has benefits and drawbacks compared to one another. Amongst these approaches, laboratory modeling stands out with its ability to prepare identical samples, keep external conditions under control, and measure deformations precisely. In this study, laboratory-based slope models at 1(Horizontal)/1(Vertical), 2/3, and 1/3 angles including the effects of precipitation and external loading were created. The results of these models were compared with those of the Plaxis 2D software. First, models were built using highly permeable cohesionless coarse-grained soils, and mixtures containing high plasticity clay (bentonite) at different rates were then prepared to investigate the effect of fine-grained soils on stability. Laboratory tests such as sieve analysis, specific gravity, consistency limits, Standard Proctor, and direct shear were used to assess the geotechnical index and mechanical properties of soils. Incremental surcharge loads were placed on the slope models and surface deformations, and local and general collapses under the effect of precipitation were observed. Laboratory model results highlighted that the fines content had a non-negligible effect on stability. When the slope behaviors were examined, it was observed that the models with a 1/3 slope had more severe local fractures and collapses. The stability of the slope is negatively affected when bentonite content in soil mixtures rises. The results of Plaxis 2D analysis are compatible with those of laboratory model tests and the factor of safety values obtained from Plaxis 2D range from 0.98 to 11.4.

## 1. Introduction

Geological formations, historical natural disasters, and climatic factors should all be considered while choosing the new construction location. Engineers are being forced to defy nature, though, due to population increase and a lack of appropriate development locations. Slope stability issue is one of the most common problems in geotechnical engineering [1-2]. Uncontrolled excavations and fillings, heavy rains, and pore water pressure variation, poor engineering properties of debris adversely affect the stability of slopes [3-5]. When the mechanism is thoroughly explored, it is seen that it depends on many more parameters than anticipated, such as soil class and density, fine and organic matter content, rainfall intensity-duration, surcharge load and location, slope height, and slope angle.

Precipitation, which increases the water content, degree of saturation, and total body weight of the soil and decreases the negative pore water pressures for unsaturated soil, adversely affects the stability of the slope [6-10]. Rainwater infiltration produces wet front formation, an increase in groundwater level, and a consequent increase in pore water pressure. This causes the soil to lose its shear strength and even causes the slope to collapse. There are many numerical and experimental studies on the effect of precipitation infiltration on slope stability [11-14]. Genc [11] mixed kaolin and bentonite clays in certain ratios (95/5, 90/10, 85/15, 80/20, 75/25, 70/30) and determined the geotechnical index and swelling properties of the obtained mixtures. According to the experimental results, it was determined that the swelling percentage increased as the bentonite ratio increased. It was also observed that the swelling index decreased with

### \* Corresponding Author

(merttakci@hotmail.com) ORCID ID 0000-0002-2261-3524

(inci.develioglu@ikcu.edu.tr) ORCID ID 0000-0001-6594-8095

(hfirat.pulat@ikcu.edu.tr) ORCID ID 0000-0002-8298-7106

(hasanemre.demirci@ikcu.edu.tr) ORCID ID 0000-0001-6455-9100

### Cite this article

Takci, M., Develioglu, İ., Pulat, H. F., & Demirci, H. E. (2023). Laboratory modeling and analysis of slopes of different geometry under the effect of precipitation. Turkish Journal of Engineering, 7(4), 349-357

increasing water content. It was observed that as the amount of bentonite increased, the liquid limit and plasticity index increased linearly, and the percentage of swelling increased as the bentonite ratio increased [11].

In this study, it was determined that the bentonite ratio, the swelling percentage in the ground and the liquid limit values were increased. In this study, the effect of this relationship on slope stability was examined.

Pınarlık et al. [12] conducted seepage analyses for the most comprehensive slope stability and steady-unsteady flow conditions of slopes, embankments, dams, and retaining walls with different soil properties with Slide V6 balance software. The program helps to determine the effects of individual variables in slope stability on the factor of safety (FS) of slope. In the study, samples with and without geotextiles with the same slope angles were analyzed by the limit equilibrium method. Soil deformations and safety coefficients occurring in both analyzes were compared. The contribution of geotextiles to the increase of soil-bearing capacity has been examined. As a result of the study, it was interpreted that the FS increased as the cohesion and the internal friction angle value increased, and it was reported that the FS of the slopes reinforced with geosynthetics reached to the safe side.

Ün [13] performed pile analysis, and modeling, on drained and undrained soils with Plaxis 2D software. According to the findings of the analysis, the FS reduced as slope height and load rose, whereas it increased when soil strength parameters increased. Additionally, it was shown that the FS rose in the model built with two-layered soil as the layer height of the soil with high shear strength grew.

Zhao et al. [14] have modeled and analyzed the excavation process of high and steeply inclined slopes in Plaxis 2D software. It has been determined that the inner rock mass affected by the excavation creates tensile stress in some areas, which is reflected in the stress distribution. Considering the unloading effect of the excavated place, it was determined that the FS of the slope gradually decreased due to the increase in the excavation depth. For this reason, it was suggested that numerical simulation should adequately account for the degradation of the rock mass caused by the excavation.

In this study, the behavior of slopes in different geometries under the influence of precipitation and surcharge loading was examined. Besides, slope stability analyses were executed by considering laboratory modeling and obtained results were compared. Observations were made about the movement mechanisms of the slopes under the influence of precipitation. It was determined to what extent the percentage of fines, angle of slope, and the amount of external loading affected the stability.

## 2. Material and Method

### 2.1. Sand

The sand used in this study was obtained from a private company and its geotechnical and mechanical

properties are shown in Table 1. After considering the geotechnical properties, the soil is classified as poorly graded silty and gravelly sand according to the Unified Soil Classification System (USCS).

**Table 1.** Geotechnical and mechanical properties of sand

| Parameter                                | Unit              | Value |
|--|-------------------|-------|
| Specific gravity ( $G_s$ )               | -                 | 2.77  |
| Plastic limit (PL)                       | %                 | NP    |
| Optimum water content ( $w_{opt}$ )      | %                 | 10.6  |
| Maximum dry density ( $\gamma_{d,max}$ ) | kN/m <sup>3</sup> | 19.8  |
| Internal friction angle ( $\phi$ )       | °                 | 31    |
| Cohesion (c)                             | kPa               | 11.3  |
| Soil classification (USCS)               | -                 | SP    |

### 2.2. Bentonite

The bentonite is convenient in terms of API 13A Part 9 specifications used in the study provided by Karben Company. It has a high swelling capacity since it contains sodium and at least 90% montmorillonite. It complies with TS EN 13500 Part 9 [15] bentonite specification and TS 977 Type-1 [16] standards. When mixed with water, it disperses easily and does not clump. The physical and chemical properties of bentonite are listed in Table 2.

**Table 2.** Physical and chemical properties of bentonite

| Parameter                           | Unit | Value |
|-------------------------------------|------|-------|
| Filtration                          | ml   | 15    |
| Humidity                            | %    | 10    |
| Yield point plastic viscosity ratio | -    | 3.0   |
| SiO <sub>2</sub>                    | %    | 61.28 |
| Al <sub>2</sub> O <sub>3</sub>      | %    | 17.79 |
| Fe <sub>2</sub> O <sub>3</sub>      | %    | 3.01  |
| CaO                                 | %    | 4.54  |
| Na <sub>2</sub> O                   | %    | 2.7   |
| MgO                                 | %    | 2.10  |
| K <sub>2</sub> O                    | %    | 1.24  |

### 2.3. Slope modeling system with precipitation effect

The box in which the slope model was created was composed of transparent tempered glass so that the deformations and movements that took place throughout the experiment could be observed. For this purpose, 6 mm thick tempered glass was placed in an aluminum frame and the box was formed. The connection points of the frame have been strengthened so that the system is not damaged during the placement and compaction processes. Water was transferred to the system with a flexible pipe and adjustable nozzles were used to equalize the rainfall intensity. Nozzles and flexible pipes were fixed to the metal frame on the system. In order to observe deformations and movements more accurately, 20 mm x 20 mm grids were formed on the front glass of the boxes. Moreover, red beads were located at the corner points of the slope model to determine the movement. The box was 116 cm in length, 60 cm in width, and 80 cm in height (H). The slope stability behavior observation system under the influence of precipitation and surcharge has been shown in Figure 1.

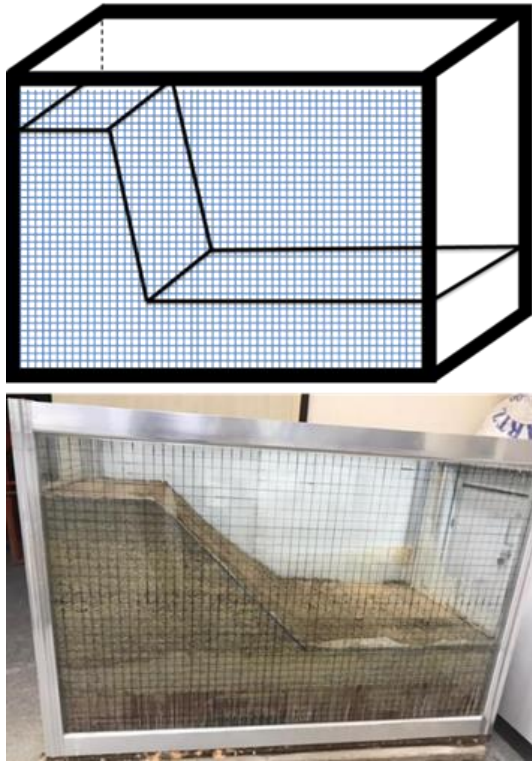


Figure 1. Slope stability behavior observation system

In the slope modeling system, the precipitation effect was created using the sprinkling method. This approach was chosen because it would provide the same quantity of water to the slope without creating deformation, as opposed to allowing droplets to develop on the surface of the slope. Instead of the physical effects of rain, it was intended to observe the impact of rainwater pressure. In this system, 4 nozzles were connected on the same flexible pipe, and water was sprayed toward the slope surface. With this system, water was supplied to the slope with a flow rate of 0.5 l/min ( $7.7 \times 10^{-3} \text{ cm}^3/\text{s}$ ). This precipitation system has been shown in Figure 2.



Figure 2. Precipitation mechanism

#### 2.4. Geotechnical index properties experiments

The grain size distribution of sand and sand-bentonite mixtures were obtained using wet sieve analysis in accordance with ASTM D422 [17] and ASTM D6913 [18]. The liquid limit was measured by the fall cone method (BS1377-1:2016) [19]. The plastic limit test was conducted by following the ASTM D4318 [20]. The soil samples were classified using consistency limits and

grain size analyses according to ASTM D2487 [21]. The specific gravity ( $G_s$ ) of samples was defined according to ASTM D854 [22]. The optimum water content and maximum dry unit weight of samples were determined with the Standard Proctor test according to ASTM D698 [23]. To determine shear strength parameters, the consolidated drained (CD) direct shear tests were conducted according to ASTM D3080/D3080M [24]. The samples were prepared at optimum water content and maximum dry unit weight. The specimens were tested in saturated conditions at three various normal stresses of 49 kPa, 98 kPa, and 196 kPa, respectively [25-27]. The test samples were sheared at a speed of 0.1 mm/min to prevent the generation of excess pore water.

#### 2.5. Slope modelling experiments

The optimum water content and 85% of the maximum dry unit weight were used while forming the slope models. The optimum water content was added to the sample, which was completely dried in an oven at 105°C for 24 hours and mixed in the concrete mixer until a homogeneous mixture was obtained. It was then compacted in layers to a thickness of 5 cm using a Standard Proctor hammer and a wooden block. The wooden block used is 58 cm long and 15 cm wide. As a result of the trial and error method, the soil placement and compaction process were performed as follows. During the compaction process, a total of 27 blows were made at 3 different points of the wooden block, with 9 blows to each point. Side and top views of the compaction process have been shown in Figure 3.

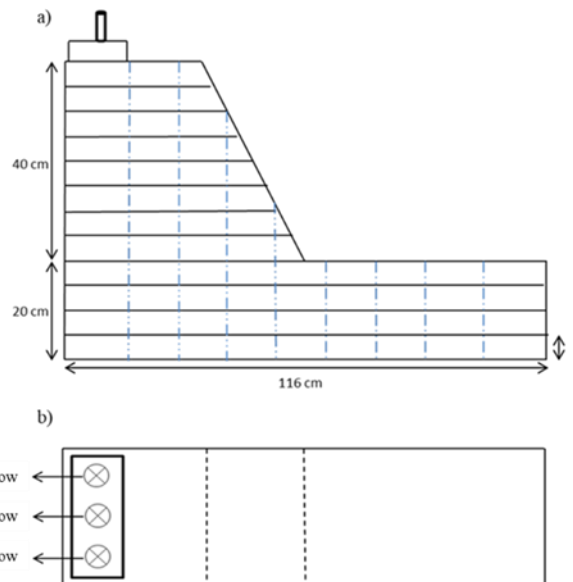


Figure 3. a) Side view of the compaction process, b) top view of the compaction process

While the sprinkler system was being installed, the annual average precipitation amount of 2021 (490 mm/m<sup>2</sup>) in the Izmir Cigli district Balatcik region was taken into consideration. These values have been obtained from the valley bulletin of the General Directorate of Agriculture and Forestry for many years [28]. By trial and error method, it was determined that while the water coming from the tap was at the maximum



level, the amount of water supplied to the system by 4 nozzles was compatible with the annual precipitation amount. A concrete block was made in the laboratory environment to transmit the surcharge load to the determined areas of the slope. These concrete blocks have dimensions of B=15 cm, L=58 cm, and H=12.5 cm. The 0.0725 m<sup>2</sup> surface of this concrete block (H x L), whose weight is adjusted as 200 N, is called the narrow area where it contacts the soil surface and the wide area when it comes into contact with its 0.087 m<sup>2</sup> surface (B x L). The surcharge load to be given to the slope was adjusted by using narrow and wide areas. The pressure values transmitted to the slope according to the narrow and large surface area have been listed in Table 3. These specified weights were loaded 6 times in total every 45 minutes and weights in the laboratory were used. The amount of bentonite in the soil was another experiment-related variable that altered. The overall goal of each experiment was to monitor the collapse state of slopes by starting with the natural soil and applying the slope's maximum effect (limited area, 1/3 slope angle, and maximum weight). Additionally, different bentonite-soil combinations of 10, 15, 20, 30, 40, and 50% were employed to compare their strengths while altering the soil's characteristics.

**Table 3.** Slope loading steps

| No | N (kg) | Higher stress         |                        | Lower stress        |                        |
|----|--------|-----------------------|------------------------|---------------------|------------------------|
|    |        | A (m <sup>2</sup> )   | P (kN/m <sup>2</sup> ) | A (m <sup>2</sup> ) | P (kN/m <sup>2</sup> ) |
| 1  | 35.5   |                       | 5                      |                     | 4.2                    |
| 2  | 71     |                       | 10                     |                     | 8.3                    |
| 3  | 142    | 0.0725                | 20                     | 0.087               | 16.7                   |
| 4  | 213    | (Narrow loading area) | 30                     | (Wide loading area) | 25.0                   |
| 5  | 284    |                       | 40                     |                     | 33.3                   |
| 6  | 355    |                       | 50                     |                     | 41.6                   |

Slope model experiments were carried out under many different geometric properties. The slope geometries used in the experiments and the names given to these models are shown in Figure 4.

**2.6. Plaxis 2D slope modelling analysis**

In order to compare the results obtained from laboratory modeling experiments with numerical analyzes, Plaxis 2D software was used for the analysis of the experiments performed in the laboratory [29]. The same geometry, dimensions, and boundary conditions were used to compare the results of the experiments with the numerical analysis. An example of the model used in the software is shown in Figure 5.

In the experiments, the soil was compressed and limited according to the optimum water content values, but a continuous sprinkler effect system was given. It is known that when the collapse state is observed, it is between the soil liquid limit and the plastic limit value. While measuring these requirements in this program, 3 analyzes were made according to the plastic limit of the soils, the liquid limit, and the water content in the optimum water content.

Mohr-Coulomb soil model was used in Plaxis 2D analysis. The values in Table 4 were used as soil parameters and were modeled as drained.

The displacement and FS values were compared by modeling and analyzing the experiments carried out in the laboratory in Plaxis 2D program. In the experiments, the soil was placed by compacting according to the optimum water content values, but the sprinkler effect was given to the system continuously. When the collapse condition is observed, it is known that the soil is between the liquid limit and the plastic limit value. For this reason, while modeling in Plaxis 2D, three different analyzes were made according to the plastic limit, liquid limit, and optimum water content of the soils.

The surcharge load given to the system in Plaxis 2D is the same as the load when the collapse condition is observed in the modeling experiment. For this reason, the results of the experiments made in the laboratory environment and the results of the analysis made in Plaxis 2D were compared.

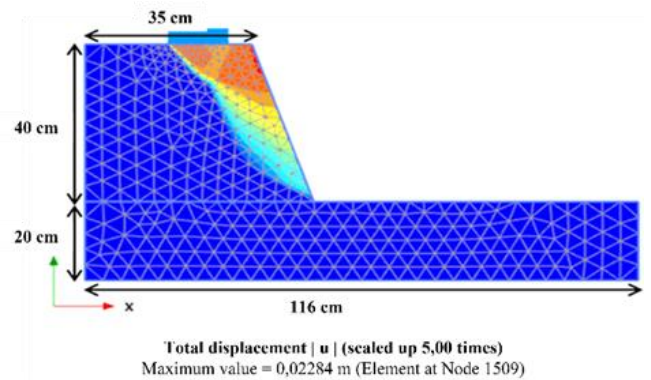


**Figure 5.** Slope model of the Plaxis 2D analysis

**3. Results**

**3.1. Results of geotechnical index properties**

The geotechnical index properties of sand and sand/bentonite mixtures are listed in Table 4. The soil classification was made according to the Unified Soil Classification System (USCS) [21].

**3.2. Results of slope modelling experiments**

In order to examine the stability behavior in detail and systematically, the parameters that will negatively affect the stability have been examined in different tests. Scenarios that will trigger instability such as increasing the angle of slope, surcharge stress, and fine-grained soil ratio have been tested in combination. As a result of many successful or unsuccessful laboratory models and examination of video recordings, slope instabilities were divided into three different classes which are punching, local deformation, and general failure. Punching deformations are comparatively smaller deformations. Although the deformations are visible to the naked eye, the raft-representative concrete block can still carry the loading plates. Local failure can be defined as a situation where significant deformations occur and the concrete plate representing the raft cannot carry the loading plates. In this case of failure, it is possible to observe a

clear slip surface, even if it is not curvilinear or circular. General failure is defined as the situation in which the greatest deformations are observed, and the concrete plate (slab) completely loses its bearing capacity. As a result of this failure, it is possible to define one or more

failure surfaces. 19 slope model experiments under various conditions such as different slope geometry and bentonite ratios were performed. Table 5 summarizes the results of slope model experiments.

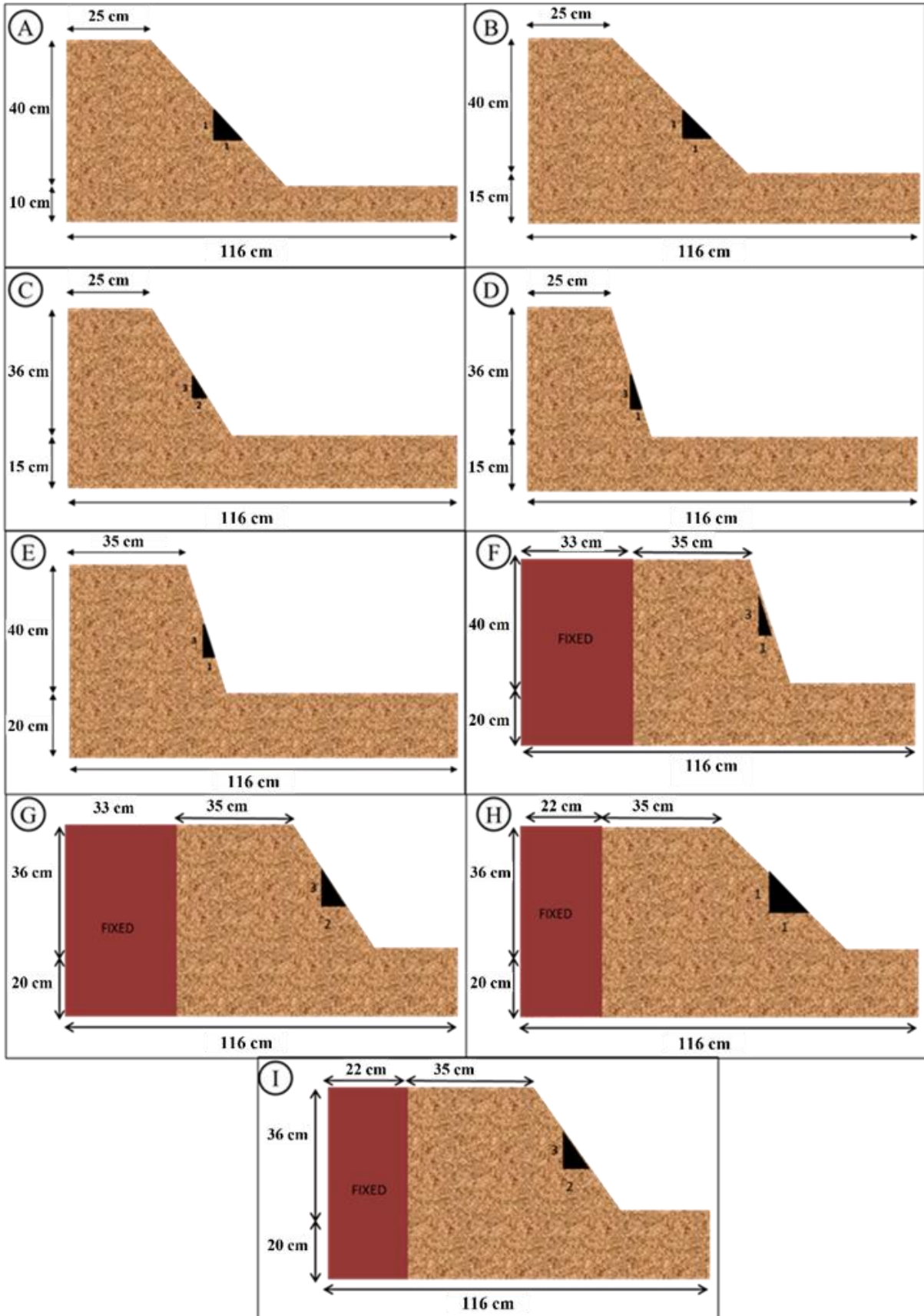


Figure 4. Geometries of slope models

**Table 4.** Geotechnical index properties of sand and sand/bentonite mixtures

| Geotechnical index properties                                | Sand | 90S  | 85S  | 80S  | 70S  | 60S  | 50S  |
|--|------|------|------|------|------|------|------|
|  |      | 10B  | 15B  | 20B  | 30B  | 40B  | 50B  |
| Max. dry unit weight, $\gamma_{drymax}$ (kN/m <sup>3</sup> ) | 19.1 | 18.6 | 18.4 | 18.1 | 17.5 | 17.5 | 17.4 |
| Optimum water content, $w_{opt}$ (%)                         | 10.6 | 10.9 | 11.3 | 13.6 | 14.5 | 15.0 | 15.8 |
| Liquid limit, LL (%)   | 16   | 43   | 80   | 92   | 98   | 118  | 142  |
| The plastic limit, PL, (%)                                   | NP   | 17   | 20   | 28   | 33   | 41   | 47   |
| Specific gravity, $G_s$                                      | 2.77 | 2.68 | 2.63 | 2.56 | 2.55 | 2.55 | 2.55 |
| $D_{10}$ (mm)  | 0.12 | -    | -    | -    | -    | -    | -    |
| $D_{30}$ (mm)  | 1.6  | 1.4  | 1.2  | 1.3  | 0.27 | -    | -    |
| $D_{60}$ (mm)  | 3.5  | 3.5  | 3.4  | 3.2  | 2.2  | 2.1  | 1.8  |
| Coefficient of uniformity, $C_u$                             | 29.2 | -    | -    | -    | -    | -    | -    |
| Coefficient of curvature, $C_c$                              | 6.1  | -    | -    | -    | -    | -    | -    |
| Soil classification, USCS                                    | SW   | SP   | SC   | SC   | SC   | SC   | SC   |
| Cohesion, $c$ (kPa)  | 11.3 | 25.9 | 30.9 | 38.3 | 48.9 | 54.0 | 55.2 |
| Internal friction angle, $\phi$ (°)                          | 31.0 | 25.7 | 21.8 | 16.6 | 12.4 | 10.2 | 10.0 |

**Table 5.** Results of slope modelling experiments

| Test No | Slope model | Slope angle (H/V) | Bentonite ratio (%) | Failure status | Failure Stress (kN/m <sup>2</sup> ) | Failure type      |
|---------|-------------|-------------------|---------------------|----------------|-------------------------------------|-------------------|
| 1       | A           | 1/1               | -                   | -              | -                                   | Punching          |
| 2       | A           | 1/1               | -                   | -              | -                                   | Punching          |
| 3       | A           | 1/1               | -                   | -              | -                                   | Punching          |
| 4       | B           | 1/1               | -                   | -              | -                                   | Punching          |
| 5       | C           | 2/3               | -                   | -              | -                                   | Punching          |
| 6       | D           | 1/3               | -                   | -              | -                                   | Local deformation |
| 7       | D           | 1/3               | 10                  | -              | -                                   | Local deformation |
| 8       | D           | 1/3               | 15                  | -              | -                                   | Local deformation |
| 9       | D           | 1/3               | 20                  | -              | -                                   | Local deformation |
| 10      | E           | 1/3               | 20                  | Failure        | 39.4                                | General failure   |
| 11      | F           | 1/3               | 20                  | Failure        | 40.8                                | General failure   |
| 12      | F           | 1/3               | 20                  | Failure        | 35.2                                | General failure   |
| 13      | F           | 1/3               | 30                  | Failure        | 33.8                                | General failure   |
| 14      | F           | 1/3               | 40                  | Failure        | 32.4                                | General failure   |
| 15      | G           | 2/3               | 40                  | Failure        | 36.6                                | General failure   |
| 16      | H           | 1/1               | 40                  | -              | -                                   | Local deformation |
| 17      | I           | 2/3               | 30                  | -              | -                                   | Local deformation |
| 18      | H           | 1/1               | 50                  | -              | -                                   | Local deformation |
| 19      | I           | 2/3               | 50                  | Failure        | 35.2                                | General failure   |

In experiment No 1, the contact area of the surcharge at the top of the slope was 0.087 m<sup>2</sup>. As a result of this experiment, no collapse was observed in the slope model. However, small punching deformations were observed under the concrete mass (Figure 6).

In experiment No 10, the angle of inclination was kept constant at 1/3 and 20% bentonite and 80% sand were used. The experiment was carried out by keeping the slope angle, precipitation intensity, loading intervals, and total load constant. The collapse was observed after approximately 3 hours and under a load of 280 kg (40 kPa) with the 80/20 sand–bentonite mixture. General failure was observed in this experiment (Figure 7). In experiment No 11, the experiment was repeated, keeping all conditions constant to check the repeatability. The results were extremely similar to the previous experiment and the modeling process proved to be reproducible.

A general failure was observed in experiment No. 12, which aimed to observe the effect of the loading period and precipitation intensity. For this reason, the rain intensity of 0.5 l/min was adjusted to 0.25 l/min. Also, loads increased every 45 minutes instead of 90 minutes.



**Figure 6.** Small deformations under the concrete mass in experiments No 1



In experiments no 13 and 14, the bentonite ratio was 30% and 40% respectively and general failures were observed. Large deformations occurred at failure stresses between 32.4 kN/m<sup>2</sup> and 33.8 kN/m<sup>2</sup>.

In experiment No. 15, the geometry was changed (G) and the angle of the slope became 2/3. General failure was observed under failure stress of 36.6 kN/m<sup>2</sup> (Figure 8). This experiment proved that a slope body that contained the same soil compositions can carry 13% more stress when the slope angle decreased from 1/3 to 2/3.



Figure 7. General failure in experiment No 10



Figure 8. General failure in experiment No 15

Soil composition did not change for experiment 16 but the slope was modeled as 1/1. Although the general failure was not observed due to the comparatively soft slope surface large deformations occurred and raft representative concrete plate did not safely carry the loading plates. In other experiments slope behavior was investigated by changing soil compositions and slope models (No.17, 18, 19). Experiments in which general failure was not observed but the concrete plate representing the raft foundation could not carry the load were defined as local failure. When the test results are compared with the literature studies, many compatible results stand out [11-13].

According to study of Genç [11], the test results showed that the swelling percentage increased as the bentonite ratio increased. It was observed that as the amount of bentonite increased, the liquid limit and

plasticity index increased linearly, and the percentage of swelling increased as the bentonite ratio increased. Therefore, indirectly, as the swelling index increases, the stability of the slope decreases [11].

### 3.3. Results of Plaxis 2D modelling analysis

Modeling and analysis of the experiments carried out in the laboratory were run with Plaxis 2D software, and the FS values were compared. In the experiments, the soil was compacted according to the optimum water content, but the precipitation effect was constantly given to the system. Therefore, when the collapse condition is observed, the soil may have a water content between the plastic limit and the liquid limit. For this reason, while modeling with Plaxis 2D software, three different analyzes were made according to the plastic limit, liquid limit, and optimum water content of the soils. Experiments were made in the laboratory with these different water contents and the internal friction angles and cohesion values were found in the results of these experiments. These values were entered into the Plaxis 2D program and the results were obtained. The surcharge load input given to the system in Plaxis 2D is the load obtained in the case of failure in the modeling experiment. Thus, the results of the experiments made in the laboratory and the results of the analysis made in Plaxis 2D could be compared. The FS values of the optimum water content, plastic limit, and liquid limit values in the analyzes of experiments No. 10, 13, 14, and 19, which were observed in the laboratory experiments, were shown in Figure 9. Although the FS value depends on the water content, it decreases as the water content increases. This shows the effect of the infiltration effect on the soil strength. But the suction values were not used during the modelling study.

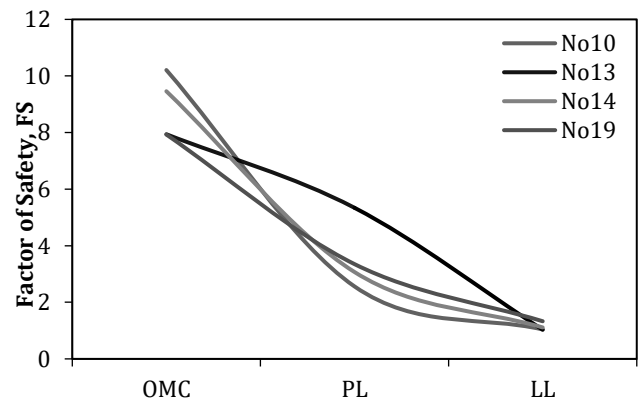


Figure 9. The FS values of the No. 10, 13, 14, and 19 experiments

The FS values of the optimum water content, plastic limit, and liquid limit values in the analyzes of experiments No 16, 17, and 18, which were not observed in the experiments performed in the laboratory, in the Plaxis 2D software, are shown in Figure 10. As mentioned above, although the FS value depends on the water content, it decreases as the water content increases.

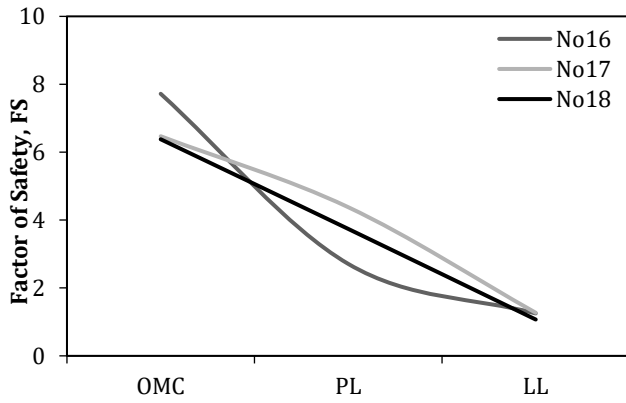


Figure 10. The FS values of the No. 16, 17, and 18 experiments

#### 4. Conclusion

This study investigated the behavior of the slope under the influence of various parameters as well as the impact of surcharge loads. Mixtures with various bentonite contents were made to investigate the effect of the fine soil ratio on the stability of the slope. Between each experiment, the slope angle was gradually changed according to the program and the slope behavior in each experiment was investigated. A sprinkler was applied along the slope surface with the fogging method at a constant flow rate to create a precipitation effect in all experiments. The findings of the study are as follows:

- Incremental surcharge loads were applied to the top of the slope at regular intervals. It is observed that as these loads increase, local deformations become more pronounced or the slope collapses.
- In slopes with the same conditions and geometry, as the bentonite ratio of the soil mixture increased, the stability of the slope was adversely affected, and the collapse of the slope became more likely.
- The collapse of the slope was observed more clearly due to the swelling property of bentonite due to the index parameters. The reason for this is that fine-grained clays have higher water retention capacity, therefore the weight of the slope body increases, and the FS decreases.
- In models under the same conditions, the weight of the slope with a small angle is greater in case of collapse. It was observed that the load at the time of failure increased by 13% when the slope angle was reduced from 2/3 to 1/3.
- When the rain intensity and loading rate are reduced by 50%, the total load in the collapsed state is 16%.
- The analysis results made in the Plaxis 2D software are consistent with the model experiments carried out in the laboratory.
- According to the analysis results obtained from the Plaxis 2D, the displacement values at the apex of the slope are approximately 9-10 times higher than the displacement values at the heel point.
- According to the analysis results obtained from the Plaxis 2D, the displacement values are the lowest in the modeling made at the optimum water content for the

same point, while the displacement value is the highest in the models made at the liquid limit water content.

- According to the graphics obtained from the Plaxis 2D, the FS value decreases as the slope angle increases, the water content of the soil increases, and the amount of bentonite in the soil increases.

#### Acknowledgement

The authors greatly acknowledge the support of the Scientific Research Project of Izmir Kâtip Celebi University (2022-TYL-FEBE-0011).

#### Author contributions

**Mert Takci:** Conceived and designed the analysis, Collected the data, Performed the analysis, writing original draft preparation; **Inci Develioglu:** Writing original draft preparation; **Hasan Firat Pulat:** Conceived and designed the analysis, Performed the analysis, writing original draft preparation; **Hasan Emre Demirci:** Contributed data or analysis tools, Performed the analysis

#### Conflicts of interest

The authors declare no conflicts of interest.

#### References

1. Das, B. M. (1994). Principles of Geotechnical Engineering. Cengage.
2. Pulat, H. F., & Yükselen Aksoy, Y. (2017). Investigation of Shear Strength and Slope Stability of Turkish Municipal Solid Waste Composition. *Teknik Dergi*, 28(1), 7703-7724
3. Yamak, S. (2017). *Karayolu şevlerinde boşluk suyu basınç değişikliklerinin şev stabilitesine etkisinin incelenmesi* (Yüksek lisans tezi, Fen Bilimleri Enstitüsü, Gazi Üniversitesi, Ankara, Türkiye).
4. Collins, B. D., & Znidarcic, D. (2004). Stability analyses of rainfall induced landslides. *Journal of geotechnical and geoenvironmental engineering*, 130(4), 362-372.
5. Griffiths, D. V., & Lane, P. A. (1999). Slope Stability Analysis by finite elements. *Geotechnique*, 49(3), 387-403.
6. Aslan Fidan, A. (2017). *Doğun olmayan koşullarda yağış infiltrasyonu etkisindeki şevlerin stabilite analizi* (Yüksek lisans tezi, Fen Bilimleri Enstitüsü, Dicle Üniversitesi, Diyarbakır, Türkiye).
7. Fourie, A. B., Rowe, D. & Blight, G. E. (1999). The effect of infiltration on the stability of the slopes of a dry ash dump. *Geotechnique*, 49(1), 1-13.
8. Gasmu, J. M., Rahardjo, H., & Leong, E. C. (2000). Infiltration effects on stability of a residual soil slope. *Computers and Geotechnics*, 26, 145-165.
9. Wersin, P., Curti, E., & Appelo, C. A. J. (2004). Modelling bentonite-water interactions at high solid/liquid ratios: swelling and diffuse double layer effects. *Applied clay science*, 26, 249-257.



10. Rocscience. (2004). A New Era in Slope Stability Analysis: Shear Strength Reduction Finite Element Technique.
11. Genç, S. (2009). Şişen zeminler ve bentonit kaolin karışımlarının şişme özellikleri, (Yüksek lisans tezi, Fen bilimleri enstitüsü, İstanbul Teknik Üniversitesi, İstanbul, Türkiye).
12. Pınarlık, M., Kardoğan, P., & Demircan, R. (2017) Şev stabilitesine zemin özelliklerinin etkisinin limit denge yöntemi ile irdelenmesi. Mühendislik Bilimleri ve Tasarım Dergisi, 5(3), 675 – 684.
13. Ün, B. (2019). Şev stabilitesi ve şev hareketlerine karşı alınacak önlemler (Yüksek lisans tezi, Fen Bilimleri Enstitüsü, Çukurova Üniversitesi, Adana, Türkiye).
14. Zhao, C., Jiang, L., Li, X., & Luo, S. (2020). Stability analysis of a rocky slope considering excavation unloading effect. The Civil Engineering Journal, 2, 170-181.
15. TS EN ISO 13500: (2006). Petroleum and natural gas industries - Drilling fluid materials - Specifications and tests. Turkish Standards.
16. TS 977 (1993). Bentonite as drilling fluid material.
17. ASTM D 422 (2020). Standard Test Method for Particle-Size Analysis of Soils ASTM International, West Conshohocken, PA, ASTM International.
18. ASTM D6913 – 04 (2009). Standard Test Methods for Particle-Size Distribution (Gradation) of Soils Using Sieve Analysis, ASTM International, West Conshohocken, PA, USA.
19. BS 1377 – 1 (2016). Methods of test for soils for civil engineering purposes. British Standard Institution, London, UK.
20. ASTM D4318 – 17e1 (2017). Standard test methods for liquid limit, plastic limit, and plasticity index of soils, ASTM International, West Conshohocken, PA, USA.
21. ASTM D2487 – 11 (2011). Standard Practice for Classification of Soils for Engineering Purposes (Unified Soil Classification System). ASTM International, West Conshohocken, PA, USA.
22. ASTM D854/D854 – 14 (2014). Standard Test Methods for Specific Gravity of Soil Solids by Water Pycnometer. ASTM International, West Conshohocken, PA, USA.
23. ASTM D698 – 12 (2021). Standard Test Methods for Laboratory Compaction Characteristics of Soil Using Standard Effort (12,400 ft-lbf/ft<sup>3</sup> (600 kN-m/m<sup>3</sup>)). ASTM International, West Conshohocken, PA, USA.
24. ASTM D3080/3080M – 11 (2011). Standard Test Method for Direct Shear Test of Soils Under Consolidated Drained Conditions. ASTM International, West Conshohocken, PA, USA.
25. Yano, K., Suzuki, M., & Nakai, T. (1997). Undrained shear and creep behavior of stiff natural clay. Conference, Japan in Deformation and Progressive Failure in Geomechanics, '97, Nagoya, 205–210.
26. Shah, K., & Shah, D. L. (2015). Interface friction between soil and geosynthetics. Proceedings of the 5th Indian Young Geotechnical Engineers Conference, March 14-15, Vadodara, Italy, 81-82.
27. Angelim, R. R., Cunha, R. P., & Sales, M. M. (2016). Determining the elastic deformation modulus from a compacted earth embankment via laboratory and Ménard pressuremeter tests. Soils Rocks, São Paulo 39(3), 285–300.
28. T.C. Çevre, Şehircilik ve İklim Değişikliği Bakanlığı, Meteoroloji Genel Müdürlüğü (2023). <https://mgm.gov.tr/>
29. Manual, T. (2016). PLAXIS 2D. Delft University of Technology & PLAXIS, Netherlands.



© Author(s) 2023. This work is distributed under <https://creativecommons.org/licenses/by-sa/4.0/>